Sensitive Detection of Halides and Nitrate in Organic and Aqueous Solvents through Selective Halogen Bonding on TTF-SAM-Modified Platinum Electrodes

Hussein Hijazi,[a] Eric Levillain,[b] Bernd Schöllhorn,*[a] and Claire Fave*[a]

This work is dedicated to the memory of the late Professor Jean-Michel Savéant.

Tetrathiafulvalene derivatives were chemisorbed on platinum electrodes. The electrochemical behavior and the stability of the resulting redox active self-assembled monolayers in the presence of various anions was studied by cyclic voltammetry. The particularly stable modified electrodes showed a high sensitivity for the detection of halides and nitrate in aprotic and aqueous solvents.

Introduction

The detection of anions, via low cost and sensitive techniques, is a major challenge that is still relevant in both environmental and medical contexts.[1] During the past years the potential of electrochemistry as a powerful tool to monitor and control anion recognition via selective halogen bonding (XB)[2] was shown in solution and at the electrode interface.[3,4] Cyclic voltammetry (CV) is an economical and precisely controllable technique, well adapted for the investigation of weak non-covalent interactions in solution. Electrochemical activation of either redox-active XB acceptors[5] or XB donors[6] showed significant and reversible XB binding enhancement upon electrochemical oxidation/reduction.

Recently, a quantitative study of electrochemically driven interfacial halogen bonding on self-assembled monolayers was described for the first time and applied to halide detection in solution.[7] Non-covalent XB was proven to be the predominant interaction in the selective anion recognition process. The halogen bond donor properties were switched on by electrochemically controlling the oxidation state of the adsorbates. The particularly high and selective binding enhancement of halide anions to the oxidized self-assembled monolayers (SAMs) could be explained by a strong surface chelate effect of the assembled 2D material on gold electrodes. In literature two other examples of XB donor containing SAMs have been reported, involving impedance spectroscopy[8] and square wave voltammetry.[9]

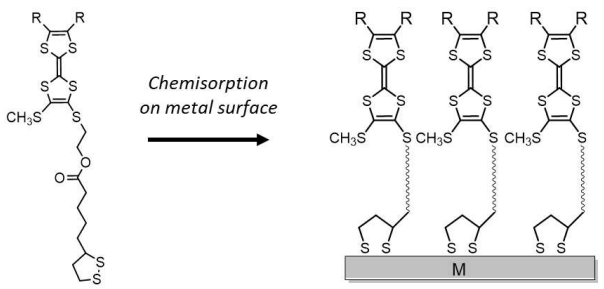
[a] *Dr. H. Hijazi, Prof. Dr. B. Schöllhorn, Dr. C. Fave*
Université Paris Cité, CNRS
Laboratoire d'Electrochimie Moléculaire
F-75013 Paris, France
E-mail: bernd.schollhorn@u-paris.fr
claire.fave@u-paris.fr
[b] *Dr. E. Levillain*
Université d'Angers
CNRS, MOLTECH-ANJOU, SFR MATRIX
49000 Angers, France

In general most organosulfur based redox-active SAMs have been studied on gold,[10] commonly considered being one of the most adapted substrates for this purpose. However, the often low stability of the monolayers is a serious limitation for their use as reproducible and re-usable sensors devices. Only few publications have reported on Pt-SAMs despite the observation of a stronger Pt–S bond compared to gold.[11] In the present study thioctic tetrathiafulvalene (TTF) derivatives were self-assembled on Pt electrodes and their electrochemical and supramolecular properties in the presence of anions were studied and compared with analogous Au-SAMs. The work focuses also on the sensitivity of the detection of halides and weakly Lewis basic anions such as nitrate.

Results and Discussion

Electrochemical behavior of the SAM

Bare Pt disc electrodes (diameter 1.6 mm) were exposed for 24 hours to a 1 mM solution of compound **1** or **2** in acetonitrile (ACN), and carefully rinsed before electrochemical characterization (Scheme 1). CVs of the resulting modified electrodes **Pt-**



1: R = I
2: R = SCH_3

M-SAM-1: R = I; M = Au, Pt
M-SAM-2: R = SCH_3; M = Au, Pt

Scheme 1. Formation of TTF SAMs on gold and platinum electrodes.

SAM-1 and **Pt-SAM-2** (Figure S1) in an electrolyte solution 0.1 M NBu_4PF_6 in acetonitrile, show a similar behavior (Figure 1A) compared to the previously described Au electrodes.[7] For **Pt-SAM-1**, two reversible and one-electron waves centered at $E^{\circ\prime}_1 = +0.73$ and $E^{\circ\prime}_2 = +0.99$ V (*vs* SCE) were attributed respectively to the formation of the corresponding radical cation and dication species (Table 1).

Analysis of the anodic and cathodic peak currents as a function of the scan rate displayed a linear dependence (Figure S2), characteristic of an electrode-surface confined electroactive species.

The electrode coverage was determined by integrating the area of the cathodic peak of the first oxidation wave and given by the equation $\Gamma = Q/nFA$, with n being the number of electrons transferred during the redox process, F the Faraday's constant and A the area of the electrode.

The coverage of **Pt-SAM-1** and **Pt-SAM-2** were found to be $1.6 \cdot 10^{-10}$ mol.cm^{-2} and $1.5 \cdot 10^{-10}$ mol.cm^{-2}, respectively. These surface concentrations are very close to those obtained previously for **Au-SAMs** with the adsorbates **1** and **2** (Table 1).[7] The experimentally determined high surface density of the SAMs strongly suggests a classic alignment of the molecules with the terminal TTF moieties being situated at the periphery as shown in Scheme 1. However, the orientation of the molecules is inferred based on previous reports in the literature[1] and without further characterization of the present system.

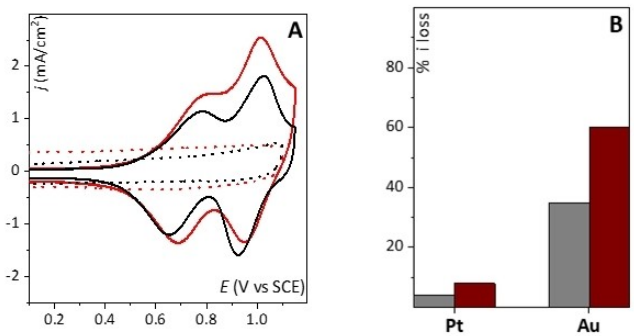


Figure 1. A) CVs of the modified electrodes (solid lines) recorded in 0.1 M NBu_4PF_6/ACN, $\nu = 10$ V/s. **Pt-SAM-1** (black trace) and **Au-SAM-1** (red trace). The corresponding CVs of the bare electrodes (Pt and Au) in the same conditions are represented with the dotted lines. **B**) **Pt-SAM-1** and **Au-SAM-1**: signal decrease after CV cycling at $\nu = 0.5$ V/s. (Grey: scanning only on the first oxidation wave and red: scanning on both waves).

Table 1. Electrochemical data for self-assembled compounds **1** and **2** on Au and Pt working electrodes in 0.1 M NBu_4PF_6/ACN.

		1st wave TTF/TTF$^{+\bullet}$		2nd wave TTF$^{+\bullet}$/TTF^{2+}	
	Γ[a]	$E^{\circ\prime}$[b]	FWMH[c]	$E^{\circ\prime}$[b]	FWMH[c]
Au-SAM-1	1.2 ± 0.1	0.72	165 ± 12	0.98	127 ± 2
Au-SAM-2	1.9 ± 0.1	0.58	155 ± 3	0.89	115 ± 1
Pt-SAM-1	1.6 ± 0.1	0.73	171 ± 1	0.99	130 ± 4
Pt-SAM-2	1.5 ± 0.1	0.60	157 ± 9	0.90	119 ± 3

[a] in 10^{-10} mol.cm^{-2}. [b] in V vs SCE. [c] in mV.

The observed deviations of the full width at half-maximum (FWHM) of the CV signals from the theoretical value (90 mV) confirmed the strong intermolecular interactions between the electroactive entities of the densely packed SAM (Table 1).[12] Interestingly, **Pt-SAM-1** exhibits a significantly higher stability over **Au-SAM-1** reflected by its higher resistance to desorption upon CV cycling at relatively slow scan rates. For instance, at 0.5 V/s, an important current intensity decrease of the peaks corresponding to first wave (TTF/TTF$^{+\bullet}$) of **Au-SAM-1** has been noticed, suggesting a significant desorption of the immobilized compound (Figure 1B).

In contrast, **Pt-SAM-1** was almost not affected, even when probing a larger potential window involving both oxidation waves. The current intensity loss of only 8% is negligible compared to 60% for **Au-SAM-1**. Such a remarkable stability of sulfur-based SAMs on Pt has already been reported in literature[13] and was attributed to the stronger binding energy of the Pt–S bond of 56 to 60 kcal/mol[14] in comparison to 40 to 50 kcal/mol[15] for the Au–S bond. This significant gain in stability was one determining argument for choosing Pt as electrode material in the present study.

A second reason was the higher overpotential of halide oxidation on Pt compared to Au. The peak potential for the irreversible chloride oxidation on a bare Au electrode was measured at +0.40 V (vs SCE), probably due to adsorption, in contrast to +0.87 V on Pt (Figure S3). At concentrations higher than 0.2 mM a significant increase of the faradaic current intensity was observed at 0.6 V on **Au-SAM-1** electrodes, partially masking the wave attributed to the TTF/TTF$^{+\bullet}$ redox couple. SAM defects are likely to account for direct chloride oxidation. This phenomenon was not observed in the case of **Pt-SAM-1** electrodes certainly due to the higher overpotential on Pt (470 mV difference).

Chloride detection on SAM modified Pt electrodes

First we focused on the detection of chloride in ACN, recognized as a particularly strong XB acceptor. When using the **Pt-SAM-1** electrode a new CV wave at lower potential emerged upon addition of tetrabutylammoniun chloride (Figure 2B). This

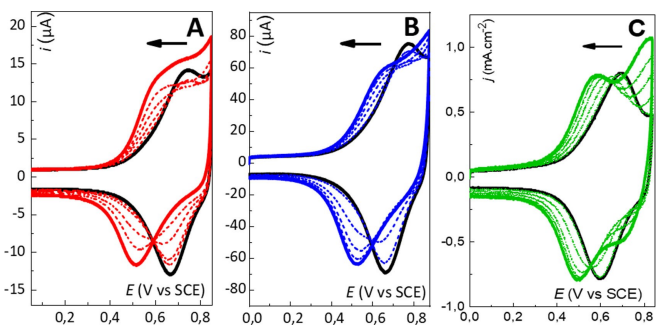


Figure 2. CVs obtained in 0.1 M NBu_4PF_6 containing solution in the presence of increasing amounts of NBu_4Cl (concentration: 0.01, 0.05, 0.1, 0.15 and 0.2 mM. CVs of **A**) **Au-SAM-1** in ACN; **B**) **Pt-SAM-1** in ACN and **C**) **Pt-SAM-1** in CH_2Cl_2. $\nu = 10$ V/s.

behaviour is similar to the reported properties of **Au-SAM-1** (Figure 2A). **Pt-SAM-2** served a reference system. It does not contain neither XB donor nor any potential HB donor sites because of the absence of halogen atoms and the presence of the thiomethyl groups. As expected, no significant perturbations were recorded with the **Pt-SAM-2** upon chloride addition (Figure S4).

The CVs of **Pt-SAM-1** at different chloride concentrations displayed a so-called "two wave behaviour": the intensity of the initial peak, corresponding to the first redox couple TTF/TTF$^{+\bullet}$, decreased progressively with increasing chloride concentration. Concomitantly, a new wave emerged at lower potential (Figure 2B). This behaviour is attributed to the presence of two distinct states of the electro-active SAM: the free TTF$^{+\bullet}$ moieties and the halogen bonded complex [TTF$^{+\bullet}$, Cl$^-$], the ratio depending on the chloride concentration (Figure 3). Consequently, the interconversion of both states via chloride exchange must be considerably slower than the time scale of the CV experiment ($\nu = 10$ V/s), otherwise a progressive shift of the oxidation wave would have been observed. For both systems, on Au and on Pt, an isopotential point was observed at ca. +0.6 V in ACN. Negative shifting of the standard potential is consistent with the effect of injecting electron density in the vicinity of the oxidized redox centre, suggesting a strong stabilization of the TTF$^{+\bullet}$ species thanks to XB interactions with chloride anions.[6a] The observed "two wave behaviour" points also to a strong binding enhancement (Binding Enhancement Factor = BEF = K_{ox}/K_{red} according to the square scheme of Figure 4) being considerably higher in magnitude compared to the analogous TTF XB donors in homogeneous solution.[6] A plausible explanation consists in the behaviour of the SAM as a chelating polytopic XB donor in contrast to the monomeric donors in solution. When increasing the chloride concentration to 0.2 mM both SAM-1 modified metal electrodes, Au and Pt, showed a consistent potential shift of $\Delta E^{\circ\prime}_1 = -134$ mV for **Au-SAM-1** and −160 mV for **Pt-SAM-1** and indicating similar binding enhancements (BEF) of 565 and 675, respectively. The BEF was calculated according to a previously reported approach based on a Langmuir isotherm through electrochemical simulations with the KISSA-1D© software.[7] When using the relationship $\Delta E^{\circ} = (RT/nF)\ \ln (K_{ox}/K_{red})$ derived from the Nernst equation, values with the same tendency were obtained, indicating a significantly higher BEF for **Pt-SAM-1** (565) than for **Au-SAM-1** (202) at 293 K, with R being the *universal gas constant*, F the *Faraday constant* and n = 1 the number of transferred electrons during the oxidation reaction. It has to be noted that neither K_{ox} nor K_{red} for a surface confined redox active receptor can be accurately determined. Up to date, no appropriate model has been reported in literature for the simulation of such materials properties at the interface with a liquid electrolyte.

The limit of detection (LOD) was determined by fitting the experimental data with a classic Langmuir adsorption model in which lateral interactions were not considered (equation 1).

$$\theta = \frac{1}{\frac{1}{K[A]} + 1} \qquad (1)$$

With θ being the fractional coverage of the respective surfaces sites, [A] the anion concentration and K the Langmuir adsorption constant. From the plot of the variation of the peak current density ($\Delta j = \theta$) depending on the chloride concentration, we could estimate the LOD for **Pt-SAM-1** versus chloride being 4.0 μM (Table 2 and Figure S5) which is close to the value recently reported for **Au-SAM-1** (LOD = 6 μM).[7]

The impact of the solvent polarity has been widely studied in the field of supramolecular chemistry and in particular for anion detection. Nowadays theoretical models of XB consider a strong electrostatic contribution.

This contribution is certainly even more pronounced for charge assisted XB as in the present case between anions and cationic XB donors such as I-TTF$^+$ moieties.

For this reason, dichloromethane (polarity index 3.1, dielectric constant 9.1) was chosen as a less polar electrolyte solvent compared to acetonitrile (polarity index 5.8, dielectric constant 37.5), in order to favour XB. The shape of CVs (Figure 2C) and surface coverage in CH_2Cl_2 (Figure S6) were similar to those recorded in ACN, standard oxidation potentials being slightly shifted towards less positive values (e.g. for **Pt-SAM-1**, $E^{\circ\prime}_1 =$

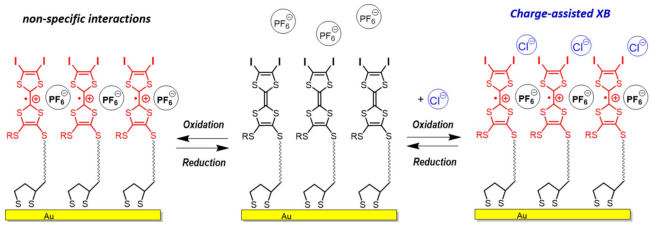


Figure 3. Scheme illustrating the surface chelate effect due to selective multiple Halogen Bonding between positively charged XB donor moieties of the oxidized **Pt-SAM-1**.

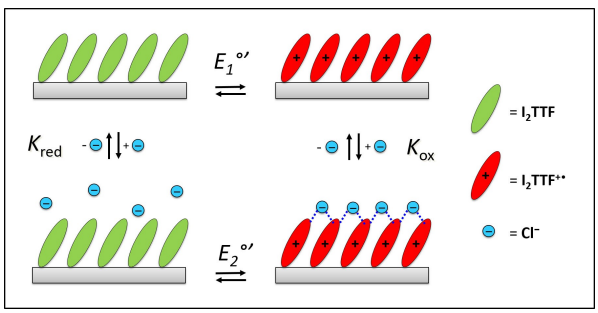


Figure 4. Electrochemical Square Scheme of **Pt-SAM-1** involving the first redox couple of the TTF adsorbate in the presence of chloride anions. For clarity, the supporting electrolyte ions are omitted.

Table 2. Shift values of the standard potential ($\Delta E^{\circ\prime}$) for the first oxidation waves of **Au-SAM-1** and **Pt-SAM-1** upon addition of 0.2 mM of NBu_4^+ salts of Cl$^-$ in 0.1 M NBu_4PF_6/ACN and the determined values for the binding enhancement factor (BEF = K_{Ox}/K_{Red}) and the limit of detection (LOD) of chloride.

	$\Delta E^{\circ\prime}$/mV	BEF	LOD/μM
Au-SAM-1	−134	565	5.9 ± 2.8
Pt-SAM-1	−160	675	4 ± 0.9

0.66 V in CH_2Cl_2 vs 0.73 V in ACN, see also Table S1). At a chloride concentration of 0.2 mM in CH_2Cl_2 the perturbation of the first oxidation wave was smaller ($\Delta E^{\circ\prime}_1 = -112$ mV) than in ACN ($\Delta E^{\circ\prime}_1 = -160$ mV) (Figures 2B and 2 C). For the second wave, potential shifts of −137 mV (CH_2Cl_2) and −67 mV (ACN) were observed, suggesting different contributions of the competing non-covalent interactions XB, π-anion and purely electrostatic interactions (Figure S7, Table S2). The nature of the solvent affected not only the intensity of the shift, but also the shape of the CVs during the titration. In both solvents an isopotential point, characteristic of a two-wave behavior, was measured only for the first wave. The LOD of chloride could be decrease by a factor of 30 from 18 μM to 0.6 μM by reducing the CV scan rate from 10 V/s to 100 mV/s, respectively (Figure S8).

As indicated above, the higher stability of Pt-SAMs compared to Au-SAMs allowed for an analysis of the second oxidation wave in the presence of chloride, thanks to reproducible experiments. After electrochemical chloride titration recording both oxidation waves within a larger potential window of 0 to 1.2 V (*vs* SCE), on a **Pt-SAM-1** a signal variation of less than 10% was observed in a chloride solution (Figure S9). The **Pt-SAMs** provided reproducible data on both redox couples TTF/$TTF^{+\bullet}$ and $TTF^{+\bullet}$/TTF^{2+}. However, in contrast to the "two wave behavior" of the first oxidation process a progressive shift was observed for the second wave upon chloride addition (Figure S7B) suggesting a faster anion exchange.

Table 3. Shift values of the standard potential ($\Delta E^{\circ\prime}$ in mV) and LOD (in μM) for the first wave of **Pt-SAM-1** upon addition of 0.2 mM of NBu_4^+ salts of Cl^-, Br^-, NO_3^-, OTf^-, ReO_4^- in 0.1 M NBu_4PF_6/CH_2Cl_2 or ACN. ν = 10 V/s

		Cl^-	Br^-	NO_3^-	OTf^-	ReO_4^-
CH_2Cl_2	$\Delta E^{\circ\prime}_1$	−112	−91	−26	−9	−9
	LOD	17.7 ± 3.0 1.26[a] 0.56[b]	6.80	0.46 ± 0.13	nd	nd
ACN	$\Delta E^{\circ\prime}_1$	−160	−135	−25	0	nd
	LOD	4.0 ± 0.9	6.2 ± 0.5	1.37 ± 0.27	nd	nd

[a] ν = 1 V/s; [b] ν = 0.1 V/s.

Selectivity and sensitivity of anion detection

Pt-SAM-1 electrodes were used for the detection of various anions in CH_2Cl_2 and in ACN (Table 3, Figure 5). For the first oxidation wave bromide showed a similar behavior as chloride with a $\Delta E^{\circ\prime}_1$ of - 91 in CH_2Cl_2 and - 135 mV in acetonitrile (Figures S10A and S11A).

The smaller potential shift compared to chloride could be explained by the weaker Lewis basicity of bromide in aprotic solvents. In acetonitrile no significant perturbation of the first oxidation wave was observed in the case of triflate and perrhenate ReO_4^- (Figures S11C) which is consistent with the considerably weaker XB acceptor strength. However, small shifts of 9 mV were recorded in CH_2Cl_2 (Figure S10).

Interestingly a consistent potential shift of ~25 mV was observed for nitrate also considered as a weak Lewis base whatever the solvent. Furthermore, a progressive shift of the oxidation wave was recorded depending on the respective nitrate concentration in contrast to the "two-wave" behavior in the presence of halides.

In order to estimate the sensitivity of the anion detection obtained with **Pt-SAM-1** electrodes the respective LOD was calculated for all studied anions showing a significant potential shift in CH_2Cl_2 or acetonitrile (Table 3). All values were found to be in the micromolar range. The only exception was observed in the case of chloride CH_2Cl_2 in with a LOD of 17 μM. However, slowing down the CV scan rate decreased the LOD by a factor of up to 30, rendering the chloride detection very sensitive.

Surprisingly extremely low LODs of around 1 μM were calculated for nitrate. Detection of these oxoanion is an overriding issue. Nitrate is one prominent constituent of acid rain and of contaminants in groundwater. To the best of our knowledge, these results represent a unique example of XB based electrochemical detection of this weak Lewis base.

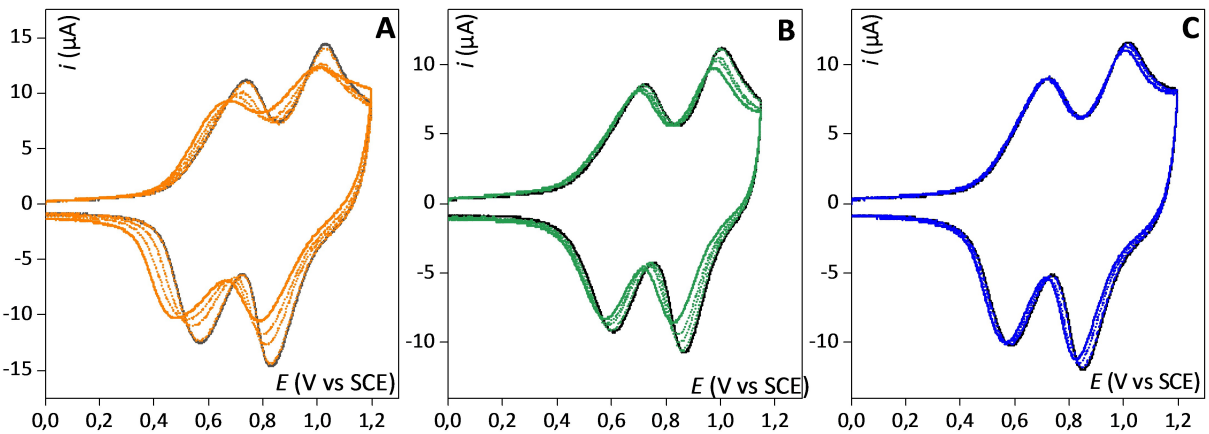


Figure 5. CVs of **Pt-SAM-1** obtained in 0.1 M NBu_4PF_6/CH_2Cl_2, in the presence of increasing amounts of **A**) Br^-, **B**) NO_3^- and **C**) ReO_4^- (concentration: 0.001, 0.05, 0.1 and 0.2 mM). ν = 10 V/s.

Anion sensing in water containing electrolytes

A decisive advantage of interfacial anion sensing is the possibility of overcoming solubility issues of the receptor and mediator molecules allowing for the analysis in aqueous electrolytes. Figure 6 shows the potential shifts recorded on **Pt-SAM-1** in the presence of Cl^-, NO_3^- and OTf^- at a concentration of 200 μM.

A consistent decrease of the potential shift was observed when adding water to the acetonitrile electrolyte. Protic solvents such as water, involve relatively strong intermolecular interactions competing with the XB donor TTF moieties as well as the employed Lewis basic anions (XB acceptors). However, HB between water and the anions is probably the most important contribution, consequently affording smaller oxidation potential shifts of the I_2TTF/ $I_2TTF^{+\bullet}$, redox couple.

In the case of chloride, a shift of 79 mV was recorded in the presence of 1% water and only 38 mV at 10% water. However, the shift values were still significant. Only two comparable examples have been published yet in literature. In a similar electrolyte (10% water/acetonitrile) no significant CV perturbation could be detected with a Ferrocene/Ferricinium based XB donor SAM on Au electrode.[9a] However, in a 1% water/acetonitrile mixture the addition of 1 mM chloride afforded a 10 mV potential shift.[9b] The LOD was not determined.

On **Pt-SAM-1** even 200 μM nitrate could be detected with potential shifts of 11 mV (1% water/acetonitrile) and 7 mV (10% water/acetonitrile) after addition of NO_3^-. The shifts were small but higher values could be observed for the second wave corresponding to the $TTF^{+\bullet}/TTF^{2+}$ redox couple with 45 mV in 1% water/acetonitrile (Table 4).

These results are very interesting and open the way to the development of sensor devices based on electrochemical XB activation as transduction mode.

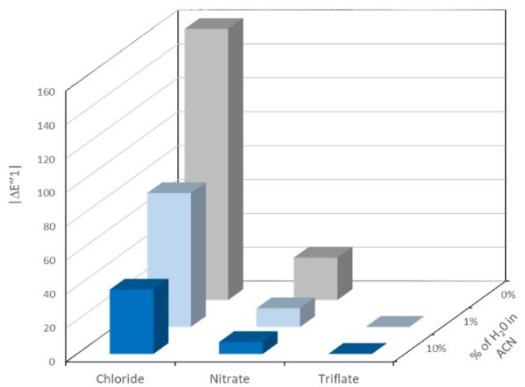


Figure 6. Shifts of the first oxidative potential $E^{\circ\prime}_1$ (in absolute value, in mV) of **Pt-SAM-1** in presence of 200 μM of various anions (Cl^-, NO_3^- and OTf^-) for various amount of H_2O (0, 1 and 10%).

Table 4. Variation of redox potential ($\Delta E^{\circ\prime}_1$ and $\Delta E^{\circ\prime}_2$ in mV) after addition of 0.2 mM of various anions (Cl^-, Br^-, NO_3^-, OTf^-, ReO_4^-) in 0.1 M NBu_4PF_6/ ACN in absence or in presence of H_2O. $\nu = 10$ V/s

	$\Delta E^{\circ\prime}_1$			$\Delta E^{\circ\prime}_2$		
	ACN	1% H_2O	10% H_2O	ACN	1% H_2O	10% H_2O
Cl^-	−160	−79	−38	−67	−61	−44
NO_3^-	−25	−11	−7	−61	−45	−10
OTf^-	−1	−1	0	−1	−3	0

Conclusion

In conclusion, the electro-active SAMs showed a significantly higher stability on Pt than on Au. This unexpected observation and the higher overpotential for the oxidation of halide anions on Pt are important aspects for the choice of the electrode material. The modified Pt electrodes were used for anion detection and particularly low LODs were determined for halide anions. Interestingly, a high sensitivity was observed also for the weakly Lewis basic nitrate anion (submicromolar LOD). Aprotic and even aqueous solvents could be successfully employed as electrolytes. Chloride was detected in the presence of weakly Lewis basic anions such as triflate and perrhenate. A similar selectivity was observed for nitrate which is a weak Lewis base itself. It was also shown that the decrease of the potential shifts with rising water content of the electrolyte did not follow the same slope for chloride and nitrate. Such different behavior could be used to determine the relative concentration of both anions simultaneously present in the solution. These interesting results confirm the high potential of immobilized electro-active XB donors for electrochemical signal transduction in molecular recognition events.

Experimental Section

Experimental details (materials, preparation of SAMs, titration experiments) are reported in the supporting information.

Acknowledgements

H. Hijazi acknowledges the French Government for his PhD. Fellowship.

Conflict of Interest

The authors declare no conflict of interest.

Data Availability Statement

The data that support the findings of this study are available in the supplementary material of this article.

Keywords: Anion detection · Halogen bonding · Molecular recognition · Pt electrodes · SAM

[1] a) J. L. Sessler, P. Gale, W.-S. Cho, J. F. Stoddart, S. J. Rowan, T. Aida, A. E. Rowan, *Anion Receptor Chemistry, The Royal Society of Chemistry*, **2006**; b) N. Busschaert, C. Caltagirone, W. van Rossom, P. A. Gale, *Chem. Rev.* **2015**, *115*, 8038–8155; c) M. S. Taylor, *Coord. Chem. Rev.* **2020**, *413*, 213270–213295; d) J. Pancholi, P. D. Beer, *Coord. Chem. Rev.* **2020**, *416*, 213281–213307.

[2] G. R. Desiraju, P. S. Ho, L. Kloo, A. C. Legon, R. Marquardt, P. Metrangolo, P. Politzer, G. Resnati, K. Rissanen, *Pure Appl. Chem.* **2013**, *85*, 1711–1713.

[3] a) C. Fave, B. Schöllhorn, Halogen Bonding in Electrochemistry, in Halogen Bonding Solution. Ed. S. Huber, Wiley, **2020**; b) C. Fave, B. Schöllhorn, *Curr. Opin. Electrochem.* **2019**, *15*, 89–96.

[4] R. Hein, P. D. Beer, J. J. Davis, *Chem. Rev.* **2020**, *120*, 1888–1935.

[5] a) S. Groni, T. Maby-Raud, C. Fave, M. Branca, B. Schöllhorn, *Chem. Commun.* **2014**, *50*, 14616–14619; b) B. R. Mullaney, M. J. Cunningham, J. J. Davis, P. D. Beer, *Polyhedron* **2016**, 20–25.

[6] a) R. Oliveira, S. Groni, C. Fave, M. Branca, F. Mavre, D. Lorcy, M. Fourmigue, B. Schöllhorn, *Phys. Chem. Chem. Phys.* **2016**, *18*, 15867–15873; b) G. Creste, S. Groni, C. Fave, M. Branca, B. Schöllhorn, *Faraday Discuss.* **2017**, *203*, 301–313; c) R. Oliveira, S. Groni, A. Vacher, F. Barrière, D. Lorcy, M. Fourmigué, E. Maisonhaute, B. Schöllhorn, C. Fave, *ChemistrySelect* **2018**, *3*, 8874–8880; d) E. Engelage, H. Hijazi, M. Gartmann, L. M. Chamoreau, B. Schöllhorn, S. Huber, C. Fave, *Phys. Chem. Chem. Phys.* **2021**, *23*, 4334–4352; e) M. A. Alvarez, C. Houzé, S. Groni, B. Schöllhorn, C. Fave, *Org. Biomol. Chem.* **2021**, *19*, 7587–7593; f) J. Y. C. Lim, M. J. Cunningham, J. J. Davis, P. D. Beer, *Chem. Commun.* **2015**, *51*, 14640–14643; g) J. Y. C. Lim, P. D. Beer, *Eur. J. Inorg. Chem.* **2017**, 220–224; h) Y. C. Tse, R. Hein, E. J. Mitchell, Z. Zhang, P. D. Beer, *Chem. Eur. J.* **2021**, *27*, 14550–14559.

[7] H. Hijazi, A. Vacher, S. Groni, D. Lorcy, E. Levillain, B. Schöllhorn, C. Fave, *Chem. Commun.* **2019**, *55*, 1983–1986.

[8] a) R. Hein, A. Borissov, M. D. Smith, P. D. Beer, J. J. Davis, *Chem. Commun.* **2019**, *55*, 4849–4852; b) S. C. Patrick, R. Hein, P. D. Beer, J. J. Davis, *J. Am. Chem. Soc.* **2021**, *143*, 19199–19206.

[9] a) S. C. Patrick, R. Hein, A. Docker, P. D. Beer, J. J. Davis, *Chem. Eur. J.* **2021**, *27*, 10201–10209; b) R. Hein, X. Li, P. D. Beer, J. J. Davis, *Chem. Sci.* **2021**, *12*, 2433–2440.

[10] a) U. Abraham, *Chem. Rev.* **1996**, *96*, 1533–1554; b) J. C. Love, L. A. Estroff, J. K. Kriebel, R. G. Nuzzo, G. M. Whitesides, *Chem. Rev.* **2005**, *105*, 1103–1169.

[11] a) R. Brito, R. Tremont, O. Feliciano, C. R. Cabrera, *J. Electroanal. Chem.* **2003**, *540*, 53–59; b) S. Sortino, S. Petralia, S. Conoci, S. Di Bella, *J. Am. Chem. Soc.* **2003**, *125*, 1122–1123; c) B. I. Rosario-Castro, E. R. Fachini, J. Hernández, M. E. Pérez-Davis, C. R. Cabrera, *Langmuir* **2006**, *22*, 6102–6108.

[12] D. Canevet, M. Sallé, G. Zhang, D. Zhang, D. Zhu, *Chem. Commun.* **2009**, 2245–2269.

[13] I. Kaur, X. Zhao, M. R. Bryce, P. A. Schauer, P. J. Low, R. Kataky, *ChemPhysChem.* **2013**, *14*, 431–440.

[14] a) H. Toulhoat, P. Raybaud, S. Kasztelan, G. Kresse, J. Hafner, *Catal. Today* **1999**, *50*, 629–636; b) O. Alexiadis, V. A. Harmandaris, V. G. Mavrantzas, L. D. Site, *J. Phys. Chem. C* **2007**, *111*, 6380–6391; c) D. Y. Petrovykh, H. Kimura-Suda, A. Opdahl, L. J. Richter, M. J. Tarlov, L. J. Whitman, *Langmuir* **2006**, *22*, 2578–2587; d) H. Toulhoat, P. Raybaud, S. Kasztelan, G. Kresse, J. Hafner, *Catal. Today* **1999**, *50*, 629–636.

[15] a) R. G. Nuzzo, L. H. Dubois, D. L. Allara, *J. Am. Chem. Soc.* **1990**, *112*, 558–569; b) J. B. Schlenoff, M. Li, H. Ly, *J. Am. Chem. Soc.* **1995**, *117*, 12528–12536; c) G. M. Whitesides, P. E. Laibinis, *Langmuir* **1990**, *6*, 87–96; d) P. E. Laibinis, C. D. Bain, G. M. Whitesides, *J. Phys. Chem.* **1991**, *95*, 7017–7021.

Manuscript received: February 19, 2022
Revised manuscript received: May 4, 2022
Accepted manuscript online: May 6, 2022